Pressure-induced decoupling of rare-earth moments and Mn spins in multiferroic GdMn_{2}O_{5}

N. Poudel, M. Gooch, B. Lorenz, C. W. Chu, J. W. Kim, and S. W. Cheong

Phys. Rev. B **92**, 144430 — Published 29 October 2015

DOI: 10.1103/PhysRevB.92.144430

Pressure-induced decoupling of rare earth moments and Mn spins in multiferroic $GdMn_2O_5$

N. Poudel[1], M. Gooch[1], B. Lorenz[1], C. W. Chu[1,2], J. W. Kim[3] and S. W. Cheong[3]
[1] *Texas Center for Superconductivity and Department of Physics, University of Houston, Houston, TX 77204, USA*
[2] *Lawrence Berkeley National Laboratory, 1 Cyclotron Road, Berkeley, CA 94720, USA and*
[3] *Rutgers Center for Emerging Materials and Department of Physics and Astronomy, Rutgers University, Piscataway, NJ 08854 USA*

The effects of pressure on the ferroelectric properties of multiferroic $GdMn_2O_5$ is studied up to 18.2 kbar. Above a critical pressure of $p_c \approx 10$ kbar, the ferroelectric transition splits into two, with the first transition shifted to higher temperature. The pressure-temperature phase diagram is derived. The results indicate a pressure-induced decoupling of the Gd moments from the Mn spin system. The conclusion is supported by thermal expansion data which show a large increase of the *c*-axis at the ambient-pressure ferroelectric transition. The pressure-induced contraction of the *c* lattice parameter is considered to be the origin of the decoupling of both magnetic subsystems above p_c.

PACS numbers: 75.30.Kz, 75.50.Ee, 75.80.+q, 77.80.-e

I. INTRODUCTION

The coexistence of multiple ferroic properties, such as magnetic and ferroelectric orders, and their coupling plays a significant role in multifunctional devices. Both experimental and theoretical researchers have been attracted in the recent years towards these materials because of the potential application in new generation devices as well as the complexity of the intrinsic microscopic interactions resulting in novel physical phenomena and properties.[1–5] The strong coupling between magnetic and ferroelectric order parameters and their mutual correlation in multiferroic compounds[3,6,7] challenges many open questions to researchers. In type II multiferroics, the inversion symmetry is broken due to unconventional frustrated magnetic orders and the polar electronic or nuclear distortions are induced through symmetric (Heisenberg) as well as antisymmetric (Dzyaloshinskii-Moriya - DM) exchange interactions.[2,5,8]

The antisymmetric DM exchange interaction is relatively small in magnitude since it arises as a relativistic effect from spin-orbit coupling. The induced polarization is therefore limited to low values. For the DM interaction to be active, a non-collinear spin structure in form of a spiral spin order is required, as observed in numerous multiferroics, e.g. $TbMnO_3$,[3] $Ni_3V_2O_8$,[9] $MnWO_4$,[10], $LiCu_2O_2$,[11] $CuFeO_2$,[12] $CoCr_2O_4$,[13] and many others.

However, the symmetric Heisenberg exchange interaction is much larger in magnitude and it occurs in collinear spin systems. If the spin system is strongly frustrated, e.g. due to competing exchange interactions or geometric constraints, an exotic magnetic structure can be stabilized which does not minimize all nearest neighbor spin exchange interactions. A typical example is the E type ($\uparrow\uparrow\downarrow\downarrow$) AFM order which has been observed in several multiferroic compounds.[14,15] The spin system tends to relax the frustration by minimizing the nearest neighbor Heisenberg exchange interaction of the energetically unfavorable spin pairs resulting in a lattice distortion which can break the spatial inversion symmetry if, for example, the neighboring ions have different charges. The cooperative distortion will induce a charge separation and an improper ferroelectric state.[2,14] This mechanism is frequently referred to as exchange striction mediated multiferroic.

Another representative of exchange striction multiferroics is the family of RMn_2O_5 (R = rare earth, Y) compounds. In the orthorhombic structure of RMn_2O_5, the $Mn^{4+}O_6$ octahedra form edge sharing chains along the *c*-axis, interlinked by bipyramidal $(Mn^{3+})_2O_8$ entities, sharing six of their eight oxygen ions with the octahedral chains. The two pyramids share one edge of their square basal plane. The rare earth ions are located in between the bipyramidal layers of Mn^{3+}. The lattice structure of RMn_2O_5 is schematically shown in Fig. 1. Geometric frustration is an inherent property of the Mn spin system since nearest neighbor Mn^{3+} and Mn^{4+} spins, correlated through antiferromagnetic (AFM) exchange interactions, form five-membered rings in a slab near the *a*-*b* plane and not all exchange interactions can be satisfied by an AFM magnetic structure. This results in a magnetic structure below a critical temperature with one pair of Mn^{3+}-Mn^{4+} per ring having nearly parallel spins. The exchange striction effect releases part of the frustration and, because of the different valences of Mn ions in the frustrated pair, results in a collaborative distortion and a macroscopic ferroelectric polarization along the *b*-axis.[16] The strong spin-lattice interaction, verified in thermal expansion[17] and scattering experiments,[18,19] mediates the polar displacement of the ions. The magnetic order of the Mn spins in the commensurate ferroelectric phase in the *a*-*b* plane is characterized by antiferromagnetic zig-zag chains made of Mn^{3+}-Mn^{3+}-Mn^{4+} repeat units stretching along the *a*-axis.[18] Two neighboring chains, offset along the *b*-axis, are coupled through pairs of Mn^{3+} and Mn^{4+} in cor-

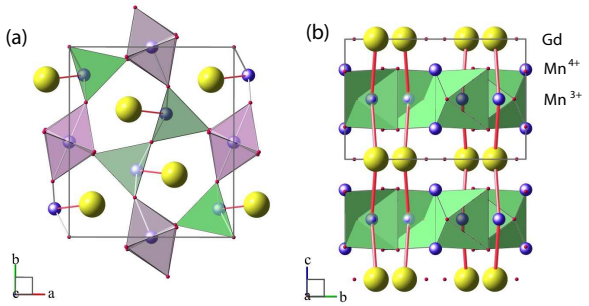

FIG. 1: Lattice structure of $GdMn_2O_5$. (a) Projection onto the a-b plane. Chains of $Mn^{4+}O_6$ octahedra run along the c-axis at the four edges of the unit cell. (b) Projection onto the b-c plane. Only the polygons defining the bipyramidal Mn^{3+} slabs are shown in (b). The red bonds connect Gd and Mn^{3+} ions forming zig-zag chains along the c-axis.

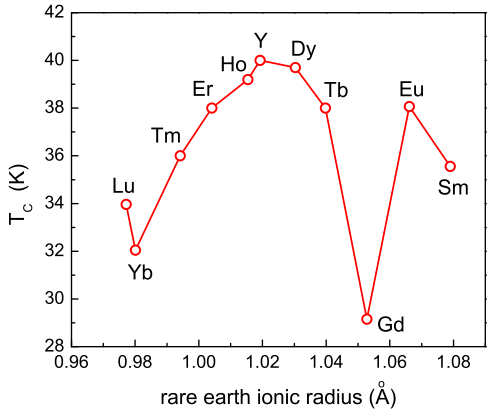

FIG. 2: Ferroelectric critical temperature of RMn_2O_5 as function of rare earth ionic radius R_{ion}. The values of T_c are extracted from original publications.[17,23,25–29]

ner sharing pyramidal and octahedral oxygen configuration, respectively. Every second interchain Mn^{3+}-Mn^{4+} pair is magnetically frustrated.[20]

As a result of the complex structure and magnetic frustration, the RMn_2O_5 compounds undergo a series of magnetic and multiferroic phase transitions upon decreasing temperature. Incommensurate magnetic order of the Mn spins sets in at the Néel temperature $T_N \approx 40$ K, followed by a transition into a commensurate magnetic structure at a slightly lower temperature T_c.[21] The commensurate phase is ferroelectric. At lower temperatures, additional anomalies in magnetic, dielectric, and thermodynamic properties indicate major changes of the magnetic system, spin reorientations induced by the anisotropy of the rare earth magnetic moment,[17] and changes of the magnetic structure back to incommensurate modulations.[18]

The ferroelectric polarization in the commensurate magnetic phase of RMn_2O_5 is of moderate size, typically a few hundred $\mu C/m^2$ to 2000 $\mu C/m^2$ in $DyMn_2O_5$.[22] However, an unusually large polarization up to 3600 $\mu C/m^2$ was recently observed in $GdMn_2O_5$.[23] The origin of the large polarization value was suggested to lie in the nearly isotropic magnetic moment of the Gd which aligns its moment antiferromagnetically with the neighboring Mn^{3+} spins via the Gd-Mn symmetric exchange interaction.[23,24] This way, the Gd moments contribute to the exchange striction process resulting in a significant increase of the ferroelectric polarization.

The correlated order of the Mn spin and Gd moment system results in a dramatic decrease of the ferroelectric transition temperature T_c in $GdMn_2O_5$, as compared to other RMn_2O_5. Fig. 2 shows the dependence of T_c on the ionic radius R_{ion} of the rare earth ion. T_c follows roughly a dome shaped dependence on R_{ion}, except for R=Gd which has the lowest T_c of all RMn_2O_5. The driving force for the commensurate order is the exchange interaction between moments of the correlated system of Mn^{3+}, Mn^{4+} spins, and Gd moments, which requires more free energy to order the complete magnetic system, thus reducing the transition temperature T_c.

Another important difference of the magnetic order in $GdMn_2O_5$ is the magnetic modulation in the commensurate phase. The incommensurate phase between T_N and T_c is characterized by a two-component modulation vector $\vec{Q}_{ICM}$=(0.49,0,0.18), similar to other RMn_2O_5 compounds. However, the commensurate phase below T_c shows only a modulation along the a-axis, $\vec{Q}_{CM}$=(0.5,0,0) with the Gd moments approximately aligned with the a-axis,[23,24] unlike other members of the family for which the z-component of $\vec{Q}_{CM}$ is different from zero (e.g. k_z=1/4 for R=Y, Ho, Tb; k_z=1/2 for R=Bi).[30] With this modulation, the closest pairs of Mn and Gd ions (distance 3.303 Å) form zig-zag chains along the orthorhombic c-axis and their respective magnetic moments are antiferromagnetically aligned. The zig-zaq chains a highlighted in Fig 1b.

External pressure can play a crucial role in tuning the dielectric and ferroelectric properties of magnetic multiferroics.[22,27,31–37] For example, theoretical calculation predicted the huge increase in polarization as well as T_N of binary magnetic multiferroic CuO to room temperature under high pressure.[38] Recently, Aoyama *et al.* reported a giant increase in polarization and switching of the direction of polarization under pressure in orthorhombic rare earth manganites[39,40]. Pressure acts in different ways than the magnetic field in multiferroics. Magnetic fields couple to the magnetic moments and affect the spin structure whereas pressure changes the bond angles and bond distances between magnetic and ligand ions which in turn affect the microscopic exchange coupling constants. As a result, external pressure may stabilize different frustrated magnetic phases. For example, a change from incommensurate to commensurate magnetic modulation, accompanied by a substantial increase of the ferroelectric polarization, was observed in other RMn_2O_5.[22,35,37] In this report we present the results of a high-pressure and thermal expansion study of $GdMn_2O_5$.

We show that pressure decouples the Mn spin and Gd moment system resulting in a two-stage ferroelectric transition. The origin of the decoupling is concluded to be the compression of the c-axis which reduces the exchange interaction between Gd moments and Mn^{3+} spins.

II. EXPERIMENTAL

The single crystals of $GdMn_2O_5$ were grown by the $B_2O_3/PbO/PbF_@$ flux method, similar to other RMn_2O_5 compounds.[26,30,41] Single crystal Laue diffraction was employed to determine and confirm the crystalline orientations. The crystal was cut perpendicular to the b-axis for dielectric and polarization measurements. Silver paint was used for electrical contacts. The contact area was 1.61 mm^2 and the sample thickness was 0.6 mm. For measurements along other directions (a- and c-axes), the crystals were cut accordingly. Hydrostatic pressure was applied in a beryllium-copper clamp cell.[42] A mixture of Fluorinert 70 and 77 liquids was used as the pressure transmitting medium. In situ pressure was measured from the change in superconducting transition temperature of high-purity lead. The sample was mounted inside a teflon container and single wires were guided out of the pressure clamp and connected to shielded cables. Because of the small section of unshielded wires, the absolute value of the sample's dielectric constant cannot be precisely determined. However, the relative changes at the magnetic and ferroelectric transitions are well defined. The dielectric properties were determined from the capacitance between the two contacts, measured by the AH 2500A capacitance bridge (Andeen-Hagerling) at a frequency of 1 kHz. The spontaneous polarization was measured through the pyroelectric current method using the K6517A electrometer (Keithley). The sample was cooled in an electric field of about 3 kV/cm to low temperature. After releasing the applied poling voltage and shortening the contacts for several minutes at the lowest temperature, the pyroelectric current was measured upon increasing temperature. The rate of temperature change was 1 K/min in all experiments. The polarization is than calculated by integrating the current from high temperature (considering no polarization in the paraelectric state) to low temperatures. Thermal expansion measurements were conducted along the a-, b-, and c-axes using a home made high-precision capacitance dilatometer.

III. RESULTS AND DISCUSSION

The dielectric constant ε_b, dielectric loss $tan\delta$, and the ferroelectric polarization P_b of $GdMn_2O_5$ at ambient pressure are shown in Fig. 3. The results are consistent with earlier reports.[23] At the onset of incommensurate magnetic order, ε_b shows an increase with a sharp slope change which defines the Néel temperature $T_N \approx 40$ K. The dielectric loss factor does not show any sizable increase at T_N which proves the purely magnetic nature of this transition. At the lower temperature $T_c = 29.2$ K, however, ε_b exhibits a sharp peak and $tan\delta$ increases rapidly, as expected near a ferroelectric phase transition. The measured electrical polarization increases below T_c and rises to about 3000 $\mu C/m^2$. It should be noted that the observed value of the polarization is lower than that reported recently,[23] which could be related to a different crystal used in the present measurements. A small hump at lower temperature ($\approx$ 11 K, labeled with a question mark in Fig. 3) observed in ε_b and $tan\delta$ indicate another minute change in the multiferroic state, however, its origin is not clear yet. A similar low-temperature anomaly of ε_b was reported previously[43] and, based on a muon spin rotation study, attributed to a transition in the Gd moment system.[44]

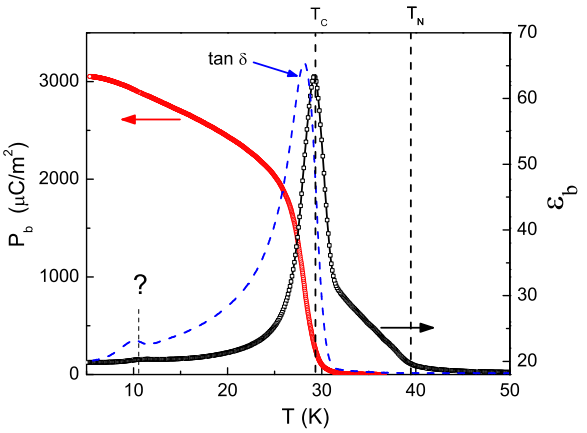

FIG. 3: Dielectric constant ε_b, loss factor $tan\delta$ (dashed line), and ferroelectric polarization P_b of $GdMn_2O_5$ at ambient pressure.

The effect of pressure on the dielectric constant is demonstrated in Fig. 4. Upon increasing pressure, the shoulder of ε_b just below T_N increases and, above 10 kbar, a second peak develops between the two critical temperatures T_N and T_c. With increasing pressure, the additional peak of ε_b becomes more pronounced and it moves to higher temperature, whereas the low-temperature peak remains and shifts slightly to lower temperature. In the following we will denote the critical temperatures of both peaks as T_{c1} and T_{c2}, respectively, as labeled in Fig. 4. The appearance of an additional peak of ε_b indicates the onset of ferroelectricity at the higher temperature T_{c2}.

The pressure dependence of the ferroelectric polarization, shown in Fig. 5, provides the proof for the enhancement of the ferroelectric temperature. Up to about 10 kbar, the polarization does not change significantly, with the onset of ferroelectricity at T_{c1} slightly decreasing with pressure. Above 10 kbar, however, a small shoulder of P_b develops at higher temperature which grows to a sizable value of 600 $\mu C/m^2$ at the highest pressure of 18.2 kbar. This value is comparable with the maximum polariza-

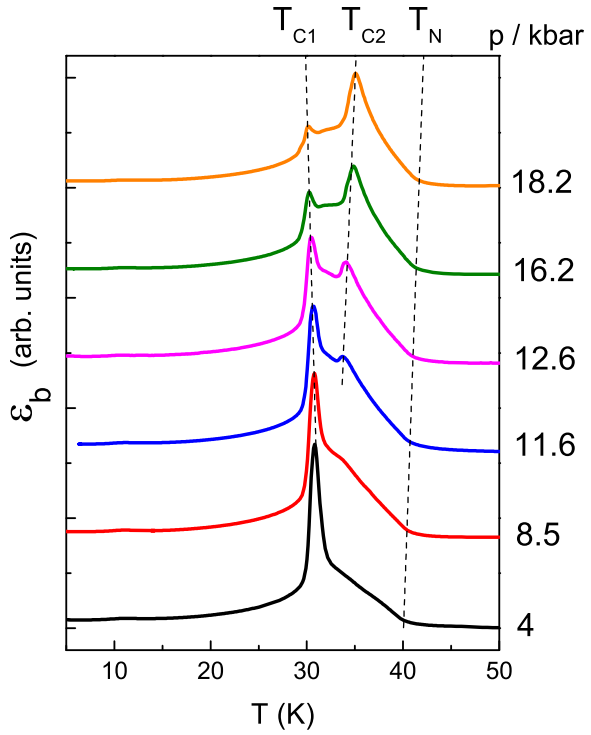

FIG. 4: Dielectric constant ε_b of $GdMn_2O_5$ at different pressures. Curves are vertically offset. The critical temperatures T_N, T_{c1}, and T_{c2} are indicated by dashed lines.

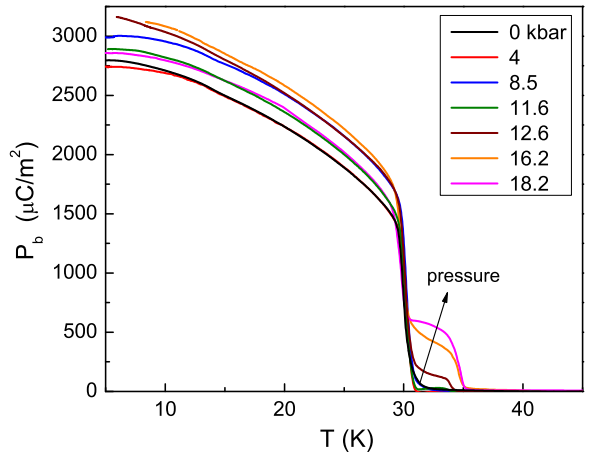

FIG. 5: Ferroelectric polarization P_b of $GdMn_2O_5$ at different pressures. The onset of ferroelectricity at T_{c2} is followed by a sharp increase of P_b at T_{c1}.

tion in other RMn_2O_5 compounds. The onset temperature, T_{c2}, quickly increases with pressure to 35 K. At the lower transition temperature, T_{c1}, P_b increases suddenly and follows approximately the temperature dependence at ambient pressure upon further cooling.

The pressure effect on the ferroelectric state in $GdMn_2O_5$ is very different from other members of the RMn_2O_5 family, where pressure did mainly increase the

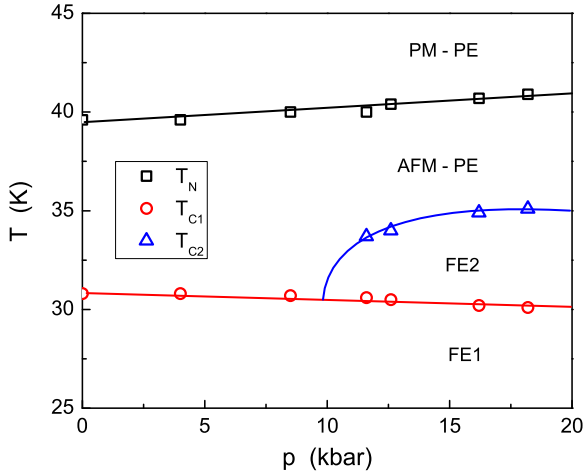

FIG. 6: Pressure-temperature phase diagram of $GdMn_2O_5$. The lines are a guide to the eye. PM=paramagnetic, PE=paraelectric, AFM=antiferromagnetic, FE=ferroelectric.

polarization in the low-temperature range by transforming the magnetic order from incommensurate to the high-temperature commensurate phase.[22,32,35,37] In $GdMn_2O_5$ the low temperature part of P_b is barely affected by pressure, but a ferroelectric phase is induced at a higher temperature, above T_{c1}. As a possible explanation of this effect, we suggest a pressure-induced decoupling of the Mn spin from the Gd moment system in the commensurate phase, allowing the Mn spins to order first at a higher transition temperature T_{c2}. The exchange striction effect of the ordered Mn spins causes the polar distortion of the same order of magnitude as in other RMn_2O_5. Only at a lower temperature T_{c1}, the Gd moments actively participate in the global magnetic order with the same inversion symmetry breaking magnetic structure, providing the additional exchange striction mechanism to increase the ferroelectric polarization further.

The pressure-temperature phase diagram is constructed from the observed anomalies of the dielectric constant and the ferroelectric polarization. Fig. 6 shows the stability ranges of different magnetic and multiferroic phases. The Néel temperature T_N increases slightly with pressure but the ferroelectric transition temperature of the FE1 phase decreases with T. Both effects can be qualitatively understood from the volume changes in passing through the transitions (see below). The high-temperature ferroelectric phase FE2 arises at about 10 kbar and T_{c2} quickly increases and tends to saturate at the highest pressure.

The exchange striction mechanism, responsible for the ferroelectric state, requires a strong spin lattice interaction giving rise to the polar lattice distortion. The ionic displacements cost elastic energy but they also gain magnetic energy by minimizing the exchange couplings between different magnetic ions. The question of which magnetic interactions are mostly affected can be

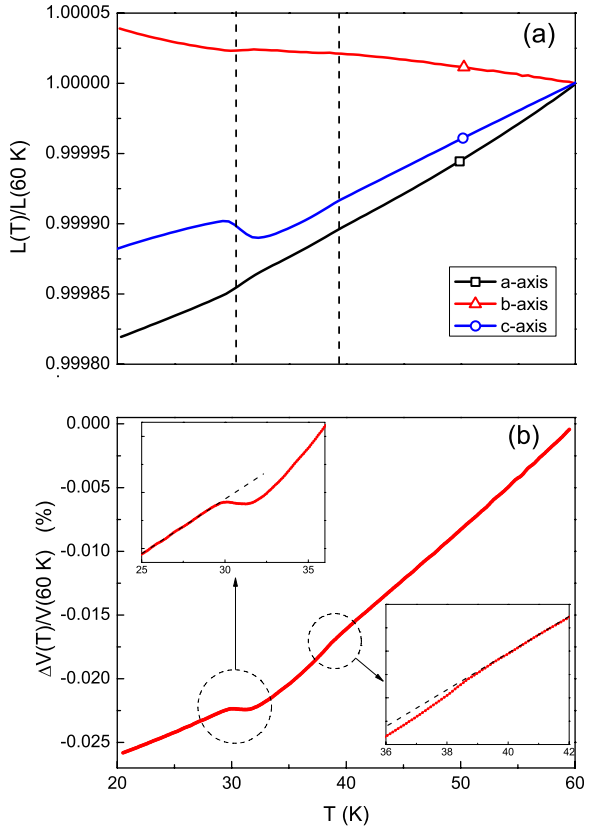

FIG. 7: (a) Relative length change along three crystallographic axes. (b) Relative volume change derived from the data in (a). The transition regions near T_N and T_c are enlarged in the lower and upper inset, respectively. The dashed lines show the extrapolation of the volume from high and low temperatures across the transitions into the incommensurate phase. The intermediate incommensurate (paraelectric) phase has a relatively smaller volume than the high-temperature paramagnetic as well as the low-temperature ferroelectric phases.

addressed by studying the macroscopic lattice changes across the ferroelectric transition in thermal expansion experiments. The results of high-precision thermal expansion measurements along all three crystallographic orientations are displayed in Fig. 7a. The relative volume change is shown in Fig. 7b.

The relative volume change across the transitions provide a qualitative determination of the pressure effects on the critical temperatures. Since the incommensurate phase has the smaller volume (as compared to the paramagnetic and ferroelectric phases, see insets in Fig. 7b), its stability range will increase under pressure. This is indeed observed in the increase of T_N and the decrease of T_{c1} (Fig. 6). More importantly, the lattice changes are strongly anisotropic at the ferroelectric transition (Fig. 7a). Whereas the lattice parameters a and b show only a subtle contraction at T_{c1}, the c-axis expands significantly at the transition into the ferroelectric phase. This expansion of c is the key to understand the relevant magnetic exchange couplings, in particular those between the Gd moments and the Mn spins.

The shortest distance between Gd and Mn ions is 3.303 Å.[25] Those short bonds are shown in the structure representation of Fig. 1 and they connect Gd with Mn^{3+} forming zig-zag chains along the c-axis (Fig. 1b) with a Gd-Mn^{3+}-Gd angle θ_{GMG}=118.6°. In the commensurate (ferroelectric) phase, the magnetic moments of the Gd and Mn^{3+} in these chains are aligned in a nearly perfect antiferromagnetic manner, according to the recent X-ray magnetic scattering study.[24] It can therefore be assumed that the antiferromagnetic exchange interaction between Gd and Mn along the chains is the most dominant one to couple both systems in the ordered state. The sizable elongation of the c-axis in the commensurate phase stretches the zig-zag chains and increases θ_{GMG}. Although details of the magnetic exchange mechanism that couples the Gd and Mn spin systems have yet to be explored, we conclude that the stretch of the zig-zag chains and the increase of θ_{GMG} provides a gain of magnetic exchange energy which further stabilizes the commensurate magnetic structure and compensates for the increase of elastic energy (including the polar distortion).

The application of pressure, however, has the opposite effect. It compresses the lattice and shrinks the c-axis which will weaken the coupling of the Gd and Mn moment systems. Above a critical pressure of 10 kbar, the Mn spin system orders below T_N at T_{c2} in the commensurate structure but the coupling to the Gd moments is not strong enough to ensure that the Gd moments participate in the long range order. The ferroelectric polarization induced by the Mn spin order increases to values of $P_b \approx 600\ \mu C/m^2$, typical for other RMn_2O_5 compounds. Only at the lower temperature T_{C1} the Gd moments participate in the magnetic order enhancing further the polar lattice distortion which increases the polarization to the highest values of $P_b \approx 3000\ \mu C/m^2$.

IV. SUMMARY AND CONCLUSIONS

We have studied the pressure effect on dielectric and ferroelectric properties of multiferroic $GdMn_2O_5$ and investigated the temperature-pressure phase diagram. Unlike other multiferroic RMn_2O_5 compounds, the application of pressure has little effect on the ferroelectric state at low temperatures. However, at higher temperatures and above a critical pressure of about 10 kbar, the ferroelectric transition splits into two. At a higher temperature T_{c2}, ferroelectricity sets in with polarization values P_b rising to 600 $\mu C/m^2$, which is typical for the commensurate Mn spin order observed in other RMn_2O_5 compounds. Upon decreasing temperature, another sudden increase of P_b at T_{c1} signals another ferroelectric transition with P_b continuously increasing to 3000 $\mu C/m^2$ at the lowest temperatures.

A second ferroelectric phase with a reduced polariza-

tion was found in several RMn_2O_5 compounds, even a sign reversal was reported in YMn_2O_5.[45] The reduction of the polarization and the sign reversal in YMn_2O_5 was suggested to originate from a competition of two contributions to the ferroelectric polarization, one arising from the exchange striction mechanism which involves the Mn^{4+}-Mn^{3+} chains (dominating in the high-temperature commensurate phase) and a second contribution due to the cycloidal spin modulation of Mn^{4+} moments along the c-axis.[46,47] The question whether or not the same mechanism could explain the pressure-induced FE2 phase in $GdMn_2O_5$ needs to be discussed in more detail.

First, it should be noted that the observed polarization drop in other RMn_2O_5 (R=Ho, Dy, Tb, Y) appeared in the low-temperature incommensurate phase and the application of pressured did enhance the polarization in this phase by transforming the incommensurate magnetic structure into the high-temperature commensurate order.[22,27,35] The ferroelectric onset temperature did only slightly increase as a function of pressure. In contrast, the pressure effect in $GdMn_2O_5$ is qualitatively different from other RMn_2O_5. The pressure-induced FE2 phase appears at higher temperature, above the ambient pressure commensurate phase. This rules out a similar mechanism involving a competition between spin current and exchange striction components to the polarization as e.g. in YMn_2O_5. Our observations rather suggest a decoupling of the Gd moment and Mn spin systems above the critical pressure which leads to an onset of commensurate Mn-spin order at a higher temperature and the Gd-moment order at lower temperature.

The proposed high-pressure phase sequence upon decreasing temperature is as follows: (i) Onset of incommensurate magnetic order (Mn spins) at the Néel temperature T_N=41 K. (ii) Onset of ferroelectricity induced by the commensurate order of the Mn spins at T_{c2}=35 K. (iii) Onset of commensurate order of Gd moments and increase of ferroelectric polarization at T_{c1}=30 K. The Gd moments and the Mn spins form an ordered structure below T_{c1} described by one complex order parameter, as suggested at ambient pressure.[23,24]

The conclusion of the pressure-induced decoupling of Gd moments and Mn spins is supported by the evaluation of the lattice response at the ferroelectric phase transition, determined through high-resolution thermal expansion measurements. We show that, at the (ambient pressure) ferroelectric transition, the c-axis expands significantly whereas a and b show only a subtle contraction. The strong response of the c-axis leads us to conclude that the main exchange couplings between the Gd and Mn spins are antiferromagnetic interactions between Gd and Mn^{3+} forming zig-zag chains along the c-axis and that the stretching of these chains results in a gain of magnetic exchange energy which is favorable in the commensurate (ferroelectric) state. Application of pressure has the adverse effect by compressing the zig-zag chains, reducing the gain in Gd-Mn^{3+} exchange energy and ultimately decoupling the Gd moment and Mn spin systems in the temperature range between 30 K and 35 K. The proposed model for the magnetic structure above 10 kbar could be verified by high-pressure magnetic scattering experiments. While neutron scattering experiments may be hampered by the strong neutron absorption of the Gd ions, X-ray magnetic scattering[24] could possibly be extended into the high-pressure range.

Acknowledgments

This work is supported in part by the US Air Force Office of Scientific Research, the Robert A. Welch Foundation (E-1297), the T.L.L. Temple Foundation, the J. J. and R. Moores Endowment, and the State of Texas through the TCSUH and at LBNL by the DoE. The work at Rutgers University was supported by the DOE under Grant No. DOE: DE-FG02-07ER46382.

[1] M. Fiebig, J. Phys. D: Appl. Phys. **38**, R123 (2005).
[2] S.-W. Cheong and M. Mostovoy, Nature Materials **6**, 13 (2007).
[3] T. Kimura, T. Goto, H. Shintani, K. Ishizaka, T. Arima, and Y. Tokura, Nature (London) **426**, 55 (2003).
[4] D. I. Khomskii, J. Mag. Mag. Mater. **306**, 1 (2006).
[5] H. Katsura, N. Nagaosa, and A. V. Balatsky, Phys. Rev. Lett. **95**, 057205 (2005).
[6] K. Taniguchi, N. Abe, T. Takenobu, Y. Iwasa, and T. Arima, Phys. Rev. Lett. **97**, 097203 (2006).
[7] N. Poudel, K.-C. Liang, Y.-Q. Wang, Y. Y. Sun, B. Lorenz, F. Ye, J. A. Fernandez-Baca, and C. W. Chu, Phys. Rev. B **89**, 054414 (2014).
[8] I. A. Sergienko, C. Sen, and E. Dagotto (2006).
[9] G. Lawes, A. B. Harris, T. Kimura, N. Rogado, R. J. Cava, A. Aharony, O. Entin-Wohlman, T. Yildirim, M. Kenzelmann, C. Broholm, et al., Phys. Rev. Lett. **95**, 087205 (2005).
[10] A. H. Arkenbout, T. T. M. Palstra, T. Siegrist, and T. Kimura, Phys. Rev. B **74**, 184431 (2006).
[11] S. Park, Y. J. Choi, C. L. Zhang, and S.-W. Cheong, Phys. Rev. Lett. **98**, 057601 (2007).
[12] T. Kimura, J. C. Lashley, and A. P. Ramirez, Phys. Rev. B **73**, 220401(R) (2006).
[13] Y. Yamasaki, S. Miyasaka, Y. Kaneko, J.-P. He, T. Arima, and Y. Tokura, Phys. Rev. Lett. **96**, 207204 (2006).
[14] Y. J. Choi, H. T. Yi, S. Lee, Q. Huang, V. Kiryukhin, and S.-W. Cheong, Phys. Rev. Lett. **100**, 047601 (2008).
[15] A. Muñoz, M. T. Casais, J. A. Alonso, M. J. Martinez-Lope, J. L. Martinez, and M. T. Fernandez-Diaz, Inorg. Chem. **40**, 1020 (2001).
[16] C. R. dela Cruz, F. Yen, B. Lorenz, S. Park, S.-W. Cheong, M. M. Gospodiniv, W. Rarcliff, J. W. Lynn, and C. W. Chu, J. Appl. Phys. **99**, 08R103 (2006).

[17] C. R. dela Cruz, F. Yen, B. Lorenz, M. M. Gospodinov, C. W. Chu, W. Ratcliff, J. W. Lynn, S. Park, and S.-W. Cheong, Phys. Rev. B **73**, 100406(R) (2006).

[18] G. R. Blake, L. C. Chapon, P. G. Radaelli, S. Park, N. Hur, S.-W. Cheong, and J. Rodriguez-Carvajal, Phys. Rev. B **71**, 214402 (2005).

[19] C. Azimonte, E. Granado, H. Terashita, S. Park, and S.-W. Cheong, Phys. Rev. B **81**, 012103 (2010).

[20] L. C. Chapon, P. G. Radaelli, G. R. Blake, S. Park, and S.-W. Cheong, Phys. Rev. Lett. **96**, 097601 (2006).

[21] P. G. Radaelli and L. C. Chapon, J. Phys.: Condens. Matter **20**, 434213 (2008).

[22] C. R. dela Cruz, B. Lorenz, Y. Y. Sun, Y. Wang, S. Park, S.-W. Cheong, M. M. Gospodinov, and C. W. Chu, Phys. Rev. B **76**, 174106 (2007).

[23] N. Lee, C. Vecchini, Y. J. Choi, L. C. Chapon, A. Bombardi, P. G. Radaelli, and S.-W. Cheong, Phys. Rev. Lett. **110**, 137203 (2013).

[24] C. Vecchini, A. Bombardi, L. C. Chapon, N. Lee, P. G. Radaelli, and C.-W. Cheong, J. Phys.: Conf. Series **519**, 012004 (2014).

[25] I. Kagomiya, K. Kohn, and T. Uchiyama, Ferroelectrics **280**, 131 (2002).

[26] N. Hur, S. Park, P. A. Sharma, S. Guha, and S.-W. Cheong, Phys. Rev. Lett. **93**, 107207 (2004).

[27] R. P. Chaudhury, C. R. dela Cruz, B. Lorenz, Y. Y. Sun, C. W. Chu, S. Park, and S. W. Cheong, Phys. Rev. B **77**, 220104(R) (2008).

[28] S. Kobayashi, H. Kimura, Y. Noda, and K. Kohn, J. Phys. Soc. Jpn. **74**, 468 (2005).

[29] Y. Koyata, H. Nakamura, N. Iwata, A. Inomata, and K. Kohn, J. Phys. Soc. Jpn. **65**, 1383 (1996).

[30] C. Vecchini, L. C. Chapon, P. J. Brown, T. Chatterji, S. Park, S.-W. Cheong, and P. G. Radaelli, Phys. Rev. B **77**, 134434 (2008).

[31] C. R. dela Cruz, F. Yen, B. Lorenz, Y. Q. Wang, Y. Y. Sun, M. M. Gospodinov, and C. W. Chu, Phys. Rev. B **71**, 060407(R) (2005).

[32] C. R. dela Cruz, B. Lorenz, M. M. Gospodinov, and C. W. Chu, J. Mag. Mag. Mat. **310**, 1185 (2007).

[33] R. P. Chaudhury, F. Yen, C. R. dela Cruz, B. Lorenz, Y. Q. Wang, Y. Y. Sun, and C. W. Chu, Phys. Rev. B **75**, 012407 (2007).

[34] C. R. dela Cruz, B. Lorenz, and C. W. Chu, Physica B **403**, 1331 (2008).

[35] C. R. dela Cruz, B. Lorenz, W. Ratcliff, J. Lynn, M. M. Gospodinov, and C. W. Chu, Physica B **403**, 1359 (2008).

[36] R. P. Chaudhury, F. Yen, C. R. dela Cruz, B. Lorenz, Y. Q. Wang, Y. Y. Sun, and C. W. Chu, Physica B **403**, 1428 (2008).

[37] H. Kimura, K. Nishihata, Y. Noda, N. Aso, K. Matsubayashi, Y. Uwatoko, and T. Fujiwara, JPSJ **77**, 063704 (2008), cond-mat/0804.3648, unpublished.

[38] X. Rocquefelte, K. Schwarz, P. Blaha, S. Kumar, and J. van den Brink, Nature Commun. **4**, 2511 (2013).

[39] T. Aoyama, K. Yamauchi, A. Iyama, S. Picozzi, K. Shimizu, and T. Kimura, Nature Commun. **5**, 4927 (2014).

[40] T. Aoyama, A. Iyama, K. Shimizu, and T. Kimura, Phys. Rev. B **91**, 081107 (2015).

[41] B. Mihailova, M. M. Gospodinov, B. Güttler, F. Yen, A. P. Litvinchuk, and M. N. Iliev, Phys. Rev. B **71**, 172301 (2005).

[42] C. W. Chu and L. R. Testardi, Phys. Rev. Lett. **32**, 766 (1974).

[43] E. I. Colovenchits and V. A. Sanina, JETP Letters **78**, 88 (2003).

[44] S. I. Vorob'ev, A. L. Getalov, E. I. Golovenchits, E. N. Komarov, V. P. Koptev, S. A. Kotov, I. I. Pavlova, V. A. Sanina, and G. V. Shcherbakov, Phys. Solid State **55**, 466 (2013).

[45] A. Inomata and K. Kohn, J. Phys.: Condens. Matter **8**, 2673 (1996).

[46] J.-H. Kim, S.-H. Lee, S. I. Park, M. Kenzelmann, J. Schefer, J.-H. Chung, C. F. Majkrzak, M. Takeda, S. Wakimoto, S. Y. Park, et al., Phys. Rev. B **78**, 245115 (2008).

[47] S. Wakimoto, H. Kimura, Y. Sakamoto, M. Fukunaga, Y. Noda, M. Takeda, and K. Kakurai, Phys. Rev. B **88**, 140403(R) (2013).